

A Multi-Scenario UAV RF Dataset with Real-World Acquisition and Signal Processing Benchmarking

Haolin Zheng¹, Ning Gao^{*1}, Zhenghang Zhu¹, Zhijun Huang²,
Shi Jin³, Michail Matthaiou⁴

¹School of Cyber Science and Engineering, Southeast University, Nanjing
210096, China

²Chien-Shiung Wu College, Southeast University, Nanjing 210096, China

³National Mobile Communications Research Laboratory, Southeast
University, Nanjing 210096, China

⁴Centre for Wireless Innovation (CWI), Queen's University Belfast, Belfast
BT3 9DT, U.K.

*Corresponding Author. Email: ninggao@seu.edu.cn

Abstract

We present a real-world multi-scenario unmanned aerial vehicle (UAV) radio frequency (RF) dataset, namely DRFF-R2, which is collected using a dedicated acquisition platform under diverse operational conditions. All signals are acquired within a unified framework to ensure consistency in hardware configuration and environmental settings. The dataset is systematically organized into seven well-defined subsets corresponding to different operational and signal composition scenarios to facilitate structured experimentation. Each file follows a clearly annotated naming convention to enable convenient data indexing and reproducible analysis. The dataset contains RF recordings from 26 UAV units spanning 8 distinct models, captured across varying flight states, altitudes, speeds, acquisition days, and receiver configurations. By covering diverse acquisition settings and signal compositions, the dataset provides a comprehensive resource for future UAV RF signal research, including RF fingerprinting (RFF) identification, model-level recognition, flight state analysis, time-varying RFF study, and interference-aware signal processing.

1 Background & Summary

The widespread adoption of low-altitude unmanned aerial vehicles (UAVs, also known as drones) across commercial, industrial, and civilian sectors has brought significant benefits to modern society. However, this rapid growth in drone deployment has also led to an increase in unauthorized and illegal activities, such as restricted airspace intrusion, illegal transportation, and privacy violations [1]. To address these concerns and ensure safe drone regulation, one promising approach is radio frequency fingerprinting (RFF), which leverages inherent hardware imperfections introduced during the manufacturing process [2]. Despite its potential, the study of drone RFF relies heavily on the extraction of unique features from drone samples,

which in turn depends on the availability of large and diverse datasets. Unfortunately, the lack of a large-scale drone radio frequency (RF) dataset presents a critical gap in this field.

Several research teams have responded to this challenge by publishing and open-sourcing their independently collected drone RF datasets. One representative dataset is DroneRFa [3], which includes RF signals from 9 types of flying drones recorded in an outdoor environment, 15 types recorded indoors, and 1 type of background signal for reference. Each dataset contains at least 12 segments, with more than 100 million sampling points per segment. Another dataset, DroneRFb [4], extended DroneRFa by focusing on non-cooperative drone control, with RF signal data from 6 different types of drones in an urban environment, as well as a reference background signal. This dataset was collected using software-defined radio (SDR) equipment and includes detailed annotations for individual identifiers, along with line-of-sight (LoS) or non-line-of-sight (NLoS) conditions. The DRFF-R1 [5] dataset comprises RF data collected from 20 UAVs across 7 different model types. The dataset covers various flight conditions, including different altitudes and velocities, and was acquired in real electromagnetic environments. It captures practical channel effects, including Doppler shifts, reflecting realistic signal propagation characteristics. The RFdrone dataset [6] offers approximately 1.3 TB of raw frequency data from 37 distinct drones, providing a comprehensive benchmark for drone detection and identification. It addresses many limitations of previous datasets by including a wide variety of drone types, large data volumes, varying signal-to-noise ratios (SNRs), and open-access evaluation tools. Additionally, the CardRF dataset [7] contains I/Q-baseband recordings of radio control and video signals from 10 consumer/prosumer drones, captured at center frequencies of 2.44 GHz and 5.8 GHz. These recordings are made in the anechoic chamber, with drones placed on a turntable to ensure consistent signal capture. And, this dataset also provides the complete hopping sequence of the control signal, and in some cases, multiple recordings for a single drone. These datasets represent important resources in advancing drone RFF research, enabling the studies of drone detection, classification, and tracking systems.

However, research on UAV RF signals has progressed beyond the classification of single drones to encompass more advanced tasks, including UAV flight state awareness [8][9][10], drone recognition under interference conditions [11][12][13][14], and the analysis of time-varying RFF characteristics [15][16]. These emerging research directions place new demands on dataset design, requiring unified data acquisition under diverse operational scenarios. Although the existing datasets provide substantial data for specific scenarios, they lack widespread coverage of diverse drone operation scenarios and systematic investigations into the various factors influencing UAV RFF characteristics. Moreover, these requirements cannot be adequately addressed by simply aggregating existing datasets, as variations in acquisition hardware, UAV models, environmental conditions, and signal configurations introduce inconsistencies that undermine cross-task comparability and unified evaluation.

To address these limitations, we collected and constructed UAV RF signals under diverse operational conditions to support a broad range of UAV RF signal research tasks, including but not limited to UAV individual identification, model recognition, flight state awareness, UAV RF signal separation and the analysis of time-varying RFF characteristics. Specifically, the dataset comprises RF signals from 26 UAV units spanning 8 distinct models and is systematically organized into seven well-defined subsets, each tailored to facilitate different research objectives and application scenarios.

2 Methods

The dataset was constructed through a controlled RF reception procedure comprising environmental baseline measurement, scenario-specific data collection and structured data storage. Data are shared under a CC-BY 4.0 license in a public repository (see Data Records section for details).

Equipment Preparation and System Configuration

The hardware components were configured and tested prior to data collection. The acquisition system consisted of the UAVs under test, RF receivers, a data storage subsystem, and auxiliary field equipment. As shown in Figure 1, all components were installed and operated according to predefined configuration settings.



Figure 1: Overall hardware architecture of the RF signal acquisition system, including UAVs, SDR-based receiver, data storage device, and auxiliary equipment.

- **UAVs:** The dataset comprises eight mainstream consumer-grade DJI drone models, totaling 26 individual airframes, as summarized in Table 1. For several models, multiple units were considered to capture intra-model variability and enhance the diversity of device-level RF fingerprint characteristics within the dataset.

Table 1: Drone platforms included in the dataset

Manufacturer	Model	Quantity
DJI	Mini 5 Pro	1
DJI	Mini 4 Pro	5
DJI	Mini 3 Pro	2
DJI	Mavic 3	1
DJI	Mavic 3C	1
DJI	Mavic Air 3S	1
DJI	Mavic Air 2S	7
DJI	Mavic Air 2	8
Total	8 Models	26 Units

- **RF Receiver:** RF signal acquisition was performed using SDR receivers consisting of two Ettus Research universal software radio peripheral (USRP) 2943 devices. The receivers support wide instantaneous bandwidth and high-rate streaming. Prior to each

acquisition session, device connectivity was checked, clock synchronization was configured, and acquisition parameters were confirmed to match predefined settings. Baseband signals were recorded under fixed hardware and configuration conditions.

- **Data Storage Subsystem:** The SDR receivers were connected to a Windows 11 laptop equipped with 16GB RAM and a 2TB external storage device. Prior to each acquisition session, buffer allocation and disk write performance were tested under the configured sampling conditions. System resource utilization was monitored during recording.

- **Auxiliary Filed Equipment:** A dual-band omnidirectional antenna with a gain of 5 dBi was used for RF signal reception. Antenna orientation, mounting height, and spatial position relative to the UAV flight path were kept constant across acquisition sessions.

For outdoor experiments, the acquisition system was deployed on a mobile workstation platform and powered by portable battery units. The power supply configuration was maintained consistently during field measurements.

- **Acquisition Software and Streaming Implementation:** Data acquisition was controlled using Python scripts developed on top of the UHD driver framework. All signal labels and associated metadata fields were predefined within the acquisition scripts and loaded automatically during recording (see Data Records section for details). Label information was written to file headers together with the corresponding signal segments. The acquisition program is publicly available at <https://doi.org/10.57760/sciencedb.36815>.

During signal acquisition, the sampling rate was fixed at $F_s = 100$ MS/s. Each acquisition segment contains approximately 1.4×10^8 complex I/Q samples. Moreover, the center frequency was configured according to the experimental scenario. For outdoor signal acquisition, a center frequency of 5.745 GHz was used. For indoor WiFi-interference signal acquisition, the center frequency was set to 2.437 GHz.

Scenario Design

Data was collected across multiple operational scenarios to capture realistic propagation dynamics and interference conditions:

1. **Ambient Noise Scenario:** Prior to UAV activation, background RF signals were recorded to characterize the baseline electromagnetic environment. These recordings serve as reference data for spectrum occupancy analysis, noise power estimation, and SNR assessment.
2. **Controlled Propagation Scenario:** Signal collection was conducted inside an enclosure lined with RF absorbing material. This configuration was used to constrain multipath propagation and external interference, thereby emulating a quasi free-space transmission condition. The recorded samples correspond to RF emissions captured under reduced environmental channel variability.
3. **Outdoor Flight Scenarios:** Controlled flight maneuvers were performed at predefined distances (e.g., 50 m horizontal separation from the receiver) and altitudes (10 m, 30 m,

and 50 m). The operational states included hovering, straight-line motion, curved trajectories, takeoff, and landing. These configurations introduce realistic propagation dynamics, including time-varying path loss, Doppler shifts due to platform motion, and multipath effects caused by surrounding structures and terrain.

4. **Indoor Interference Scenarios:** Signal collection was conducted in enclosed indoor environments with active WiFi traffic in the 2.4 GHz band. The UAV operated within the same frequency range, resulting in co-channel and adjacent-channel interference conditions. The recorded samples therefore reflect RF emissions captured under spectrally congested indoor environments.
5. **Multi-Drone Mixed Scenarios:** Multiple UAVs were operated simultaneously within the same frequency band during data collection. Concurrent transmissions resulted in partial or complete spectral overlap, time-varying power levels, and composite signal superposition at the receiver. The recorded samples therefore contain mixed RF emissions from multiple transmitters captured under shared-spectrum conditions.

Signal Acquisition Procedure

As illustrated in Figure 2, all data collection sessions followed a predefined acquisition workflow covering UAV operation, SDR configuration, and data recording.

The UAV operators were responsible for drone operation and flight-state control. Prior to recording, the UAV was powered in proximity to the receiving antenna, and a communication link was established via a calibrated remote controller or the official mobile application. Once connected, telemetry status, GPS positioning, video transmission quality, and battery level were directly monitored through the application interface to confirm stable operating conditions. The operators executed predefined UAV flight states, including hovering, linear motion, curved trajectories, takeoff, and landing, at specified distances and altitudes according to the scenario configuration.

The acquisition program operator was responsible for SDR configuration and data saving. The acquisition workstation was initialized, and the USRP device was connected and configured by using the UHD-based Python program. Key parameters, including sampling rate, center frequency, and receiver gain, were set according to the designated scenario and fixed prior to recording. During acquisition, signal quality indicators were monitored in real time to identify abnormal interference or instability. Upon completion of the current acquisition procedure, the recorded data file was saved using a structured naming convention embedding essential metadata, after which the workflow proceeded to the next predefined acquisition procedure.

3 Data Records

The dataset is publicly hosted on the Science Data Bank platform at <https://doi.org/10.57760/sciencedb.36815>. This dataset is distributed under the Creative Commons Attribution 4.0 International (CC BY 4.0) license (<https://creativecommons.org/licenses/by/4.0/legalcode>). It consists of seven directories, each containing distinct UAV RF signal data:

- `dataset1-single_drone_states`: This directory contains RF signal data captured from a single drone in various operational states, including Cruise, TakeOff, Ascend, Descend, Landing, and Shading.

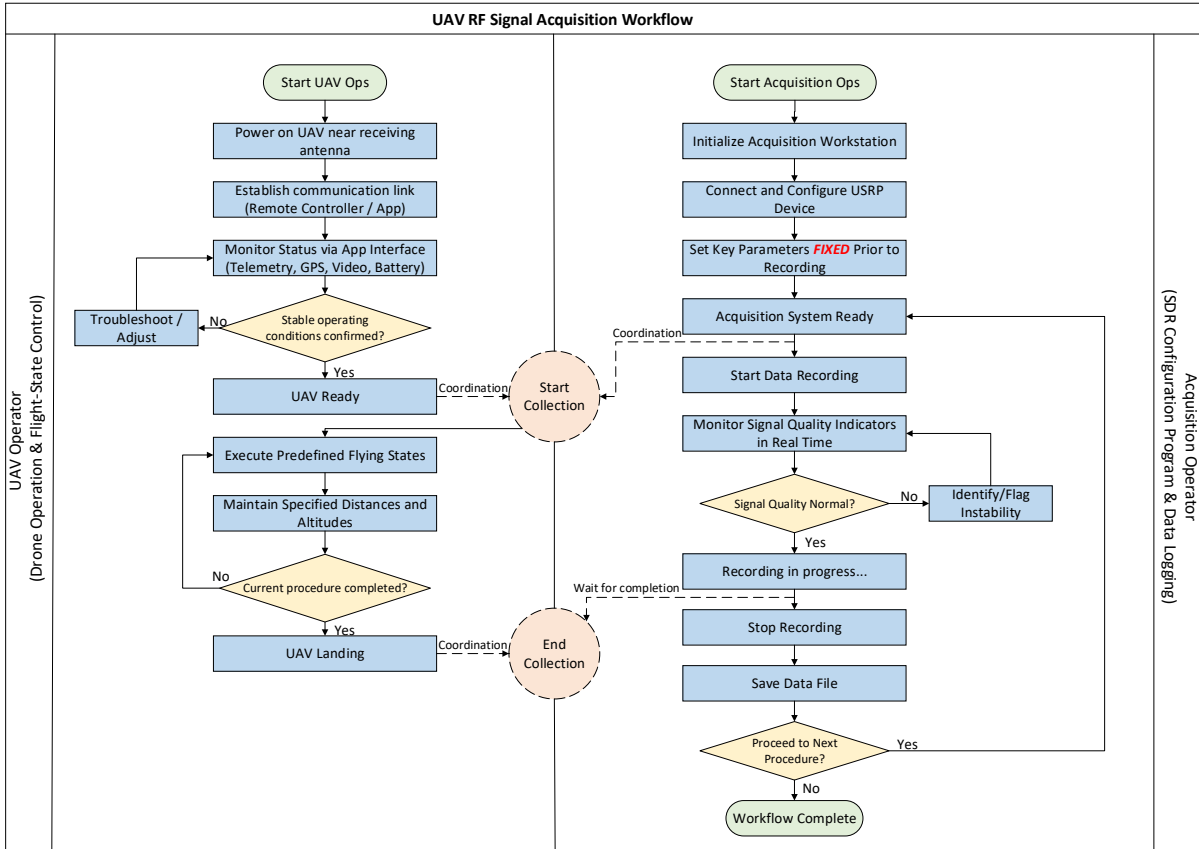


Figure 2: Standardized signal acquisition flowchart.

- `dataset2-drone_mixed`: This directory includes several subdirectories, each containing mixed RF signal data from two or three drones flying simultaneously. For example, the subdirectory `mavic_air2s_2_&mavic_air2s_3` contains signals from two individual Mavic Air 2S drones.
- `dataset3-single_drone_hover`: This directory provides data from different drones hovering at various times (e.g., Day 1, Day 2, Day 3). It also includes data captured from the same drone under different conditions, such as hovering data collected by different USRPs.
- `dataset4-single_drone_dual_frequency`: This directory contains RF signal data collected when the drone is operating in frequency hopping mode. RF signals outside this directory are assumed to be captured without frequency hopping enabled.
- `dataset5-single_drone_inside_absorbent_cotton`: This directory contains RF signal data from a drone wrapped in absorbent cotton, designed to minimize external environmental influences, thus providing cleaner drone RF signals. Additionally, the directory contains subdirectory labeled `dual_frequency_5.745&2.437` and `single_frequency_5.745`, representing the drone's signals captured with and without frequency hopping, respectively.
- `dataset6-wifi_mixed`: This directory contains RF data captured from a drone while its signals are mixed with Wi-Fi signals, enabling the study of drone signal performance in the presence of Wi-Fi interference.

- `dataset7-environment`: This directory contains environmental signal data captured prior to drone RF signal collection, providing context for external factors that might affect the drone’s signal.

The drone RF signal data are stored in MAT format. To better organize and store the UAV RF signal data, we have clearly annotated the naming format for each file. Specifically, consider the file name `mavic3_1_Ascend_c17_u1_d2.mat`:

- `mavic3_1`: Indicates the first UAV instance of the MAVIC 3 model.
- `_Ascend`: Represents the current flight state of the drone.
- `_c*`: Refers to a combination of the drone’s flight mode, speed, and state. Since the combinations vary across different dataset dictionaries, we have provided detailed information about these combinations in Table 2 for reference.
- `_u*`: Denotes the USRP number used for collecting the signal.
- `_d*`: Indicates the day on which the signal was captured.

Table 2: Description of UAV RF signal datasets and flight parameters

Dataset	Label	Alt. (m)	Speed (m/s)	Flight Maneuver	Lat. Dist. (m)	State
	c1	10	0-5	Linear Flight	50	Cruise
	c2	10	5-10	Linear Flight	50	Cruise
	c3	30	0-5	Linear Flight	50	Cruise
	c4	30	5-10	Linear Flight	50	Cruise
	c5	50	0-5	Linear Flight	50	Cruise
	c6	50	5-10	Linear Flight	50	Cruise
	c7	10	0-5	Curved Flight	50	Cruise
	c8	10	5-10	Curved Flight	50	Cruise
	c9	30	0-5	Curved Flight	50	Cruise
	c10	30	5-10	Curved Flight	50	Cruise
	c11	50	0-5	Curved Flight	50	Cruise
	c12	50	5-10	Curved Flight	50	Cruise
Dataset 1	c13	10	0	Hovering (Video)	-	Cruise
	c14	30	0	Hovering (Video)	-	Cruise
	c15	50	0	Hovering (Video)	-	Cruise
	c16	0 → 3	0-3	Take-off	30	TakeOff
	c17	3 → 50	0-5	Ascent	30	Ascend
	c18	3 → 50	5-10	Ascent	30	Ascend
	c20	50 → 3	0-5	Descent	30	Descend
	c21	50 → 3	5-10	Descent	30	Descend
	c22	3 → 0	0-3	Landing	30	Landing
	c23	10	0	Hovering (Occluded)	30	Shading
	c24	30	0	Hovering (Occluded)	30	Shading
	c25	50	0	Hovering (Occluded)	30	Shading

Continued on next page

Table 2 - continued from previous page

Dataset	Label	Alt. (m)	Speed (m/s)	Flight Maneuver	Lat. Dist. (m)	State
	c26	Mixed	0-5	Linear (Occluded)	50	Shading
Dataset 2	c1	10	0	Hovering	3	Hover
	c2	10	0	Hovering	3	Hover
	c3	30	0	Hovering	3	Hover
	c10	10	0-5	Co-directional	50	Cruise
	c11	10	5-10	Co-directional	50	Cruise
	c12	30	0-5	Co-directional	50	Cruise
	c13	30	5-10	Co-directional	50	Cruise
	c14	50	0-5	Co-directional	50	Cruise
	c15	50	5-10	Co-directional	50	Cruise
Dataset 3-5	c1	10	0	Hovering	3	Hover
	c2	10	0	Hovering	3	Hover
	c3	30	0	Hovering	3	Hover
Dataset 6	c1	5	0	Hovering	3	Hover
	c2	10	0	Hovering	3	Hover
	c4	5	0-5	Linear Flight	50	Cruise
	c6	10	0-5	Linear Flight	50	Cruise

Note: Lat. Dist. = Lateral Distance to Receiver; Alt. = Altitude.

This structured naming convention enables efficient indexing, retrieval, and organization of UAV RF data. Each filename encodes key metadata, including UAV model, operational state, acquisition scenario, and timestamp, thereby ensuring clear traceability across recording sessions. In addition to filename-level metadata, each data file contains a fixed internal structure with predefined variables as summarized in Table 3.

Table 3: Internal data structure of each acquisition file

Variable Name	Description
RF0_I	In-phase (I) component of the received signal
RF0_Q	Quadrature (Q) component of the received signal
Fs	Sampling rate (Hz)
CenterFrequency	Center frequency (Hz)
Gain	Receiver gain (dB)
State	UAV operational state label (e.g., hovering)
Distance	Horizontal distance between the UAV and the receiver
Height	Flight altitude at the time of signal recording
FlightMode	Description of the UAV flight mode

4 Technical Validation

In this section, we conduct a set of simple yet representative characterizations to demonstrate the quality, consistency, and usability of the collected UAV RF signals.

Time-Frequency Representation of RF Signals

To examine the time-frequency characteristics under different acquisition conditions, representative samples from dataset-2, dataset-3, and dataset-6 were selected for analysis. Short-time Fourier transform (STFT) representations were computed for the corresponding RF signal segments.

Let $x[n]$ denote the discrete-time complex baseband I/Q signal. The STFT is defined as

$$X(m, k) = \sum_{n=0}^{N_{\text{FFT}}-1} x[n + mH] w[n] e^{-j2\pi kn/N_{\text{FFT}}}, \quad (1)$$

where $w[n]$ is a Hann window of length $N_{\text{FFT}} = 1024$, $H = 256$ denotes the hop size, m is the time-frame index, and k is the frequency bin index. For each RF segment, a fixed duration of 0.1s is selected for time-frequency analysis to maintain uniform representation across all samples. The magnitude spectrogram is computed as

$$S(m, k) = |X(m, k)|, \quad (2)$$

and further transformed into the logarithmic domain to enhance the visibility of fine-grained spectral structures:

$$S_{\text{dB}}(m, k) = 10 \log_{10} (S(m, k)^2 + \epsilon), \quad (3)$$

where ϵ is a small constant introduced for numerical stability.

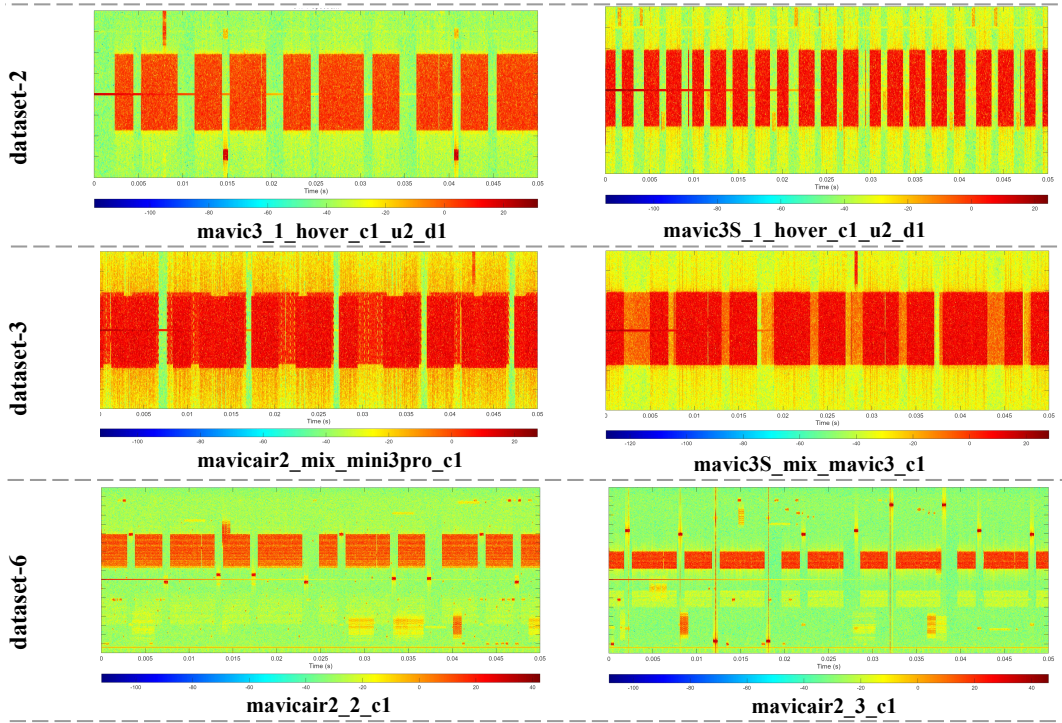


Figure 3: Representative STFT spectrogram samples from the proposed dataset under three acquisition scenarios: single-UAV hovering, dual-UAV mixed transmission, and UAV signals mixed with Wi-Fi interference.

Representative STFT spectrograms are shown in Figure 3. The corresponding time-frequency representations exhibit structured spectral patterns across scenarios, with observable differences in spectral occupancy, temporal continuity, and interference structure among distinct signal compositions. No abnormal discontinuities or saturation artifacts are observed in the analyzed segments.

Flight State Awareness Experiment

To assess label consistency and class separability, a baseline supervised classification experiment was conducted using dataset-1, which comprises RF signals from eight UAV models across 26 fine-grained operational states (c1-c26).

A convolutional neural network based on the EfficientNetB0 architecture was implemented as a reference model. Signal segments were preprocessed and used to train a multi-class classifier for state recognition. The implementation details and source code are publicly available at <https://doi.org/10.57760/sciencedb.36815>.

The confusion matrix in Figure 4 shows the distribution of predicted labels across the 26 operational states. The classification results indicate observable correspondence between the recorded RF signals and the annotated flight state labels, suggesting the presence of distinguishable RF characteristics in the dataset.

5 Data Availability

The dataset is publicly hosted on the Science Data Bank platform at <https://doi.org/10.57760/sciencedb.36815> [17], ensuring long-term preservation, accessibility, and reproducibility. This dataset is distributed under the CC BY 4.0 license.

6 Code Availability

The signal acquisition program and associated experimental code are publicly available at <https://doi.org/10.57760/sciencedb.36815>

7 Acknowledgements

This work was supported in part by the National Key Research and Development Program of China under Grant 2024YFE0200700, in part by National Science Foundation of China (NSFC) under Grants 62371131, and in part by Undergraduate Training Programs for Innovation of Jiangsu Province.

References

- [1] He, Y., Zhang, J., Xi, R., Na, X., Sun, Y. & Li, B. Detection and identification of non-cooperative UAV using a COTS mmWave radar. *ACM Trans. Sens. Netw.* **20**, 44 (2024). <https://doi.org/10.1145/3638767>

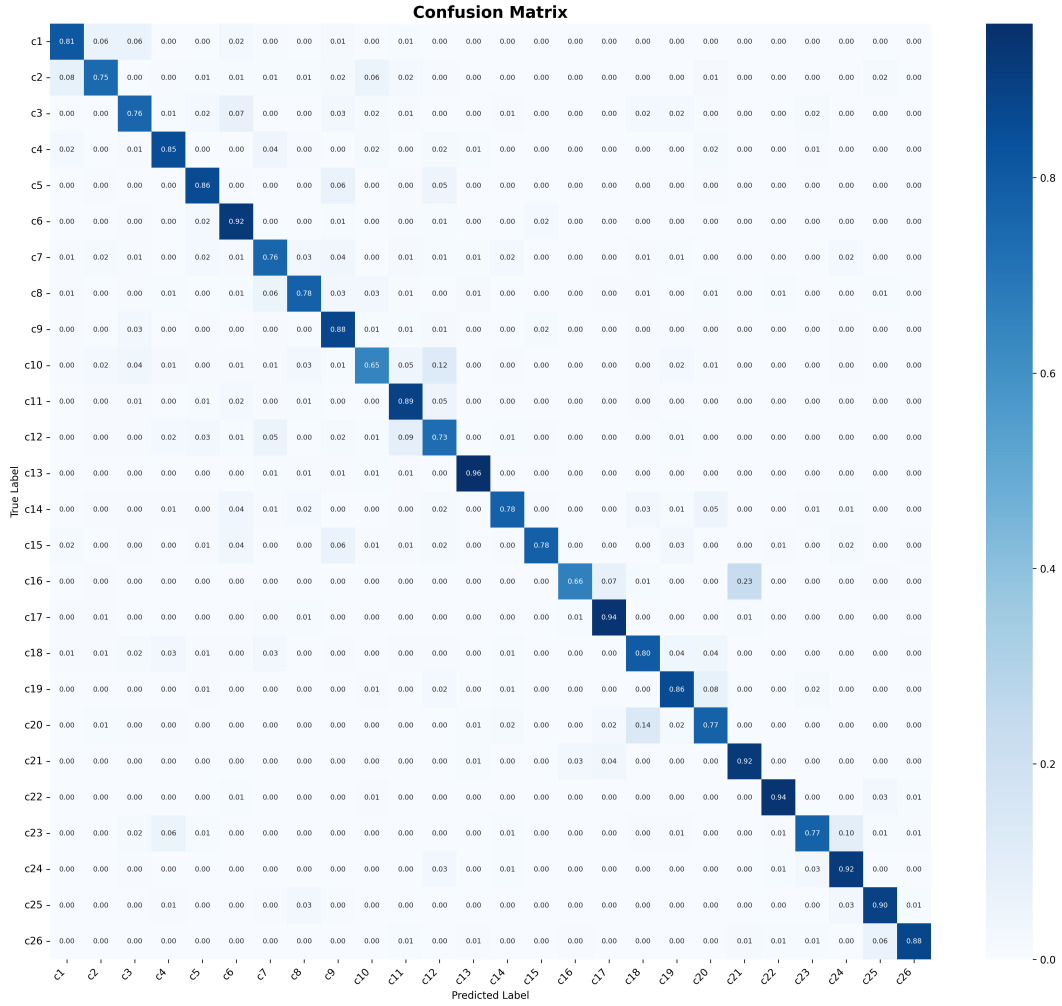


Figure 4: Confusion matrix for 26 UAV operational states (c1-c26) obtained using a baseline EfficientNetB0 classifier on dataset-1.

[2] Yang, S., Han, H., Liu, Y., Guo, W., Pang, Z. & Zhang, L. Reconfigurable intelligent surface-induced randomness for mmWave key generation. In *Proc. IEEE ICC* 2909–2914 (2023). <https://doi.org/10.1109/ICC45041.2023.10278950>

[3] Yu, N., Mao, S., Zhou, C., Sun, G., Shi, Z. & Chen, J. DroneRFa: A large-scale dataset of drone radio frequency signals for detecting low-altitude drones. *J. Electron. Inf. Technol.* **46**, 1147–1156 (2024). <https://doi.org/10.11999/JEIT230570>

[4] Ren, J., Yu, N., Zhou, C., Shi, Z. & Chen, J. DroneRFb-DIR: An RF signal dataset for non-cooperative drone individual identification. *J. Electron. Inf. Technol.* (2025). <https://doi.org/10.11999/JEIT240804>

[5] Zheng, H., Gao, N., Cai, D., Jin, S. & Matthaiou, M. UAV individual identification via distilled RF fingerprints-based LLM in ISAC networks. *IEEE Wireless Commun. Lett.* **14**, 3769–3773 (2025). <https://doi.org/10.1109/LWC.2025.3603423>

[6] Shi, R. *et al.* RFUAV: A benchmark dataset for unmanned aerial vehicle detection and identification. Preprint at <https://arxiv.org/abs/2503.09033> (2025).

- [7] Vuorenmaa, M., Marin, J., Heino, M., Turunen, M. & Riihonen, T. Radio-frequency control and video signal recordings of drones. Zenodo <https://doi.org/10.5281/zenodo.4264467> (2020).
- [8] Al-Sa'd, M. F., Al-Ali, A., Mohamed, A., Khattab, T. & Erbad, A. RF-based drone detection and identification using deep learning approaches: An initiative towards a large open source drone database. *Future Gener. Comput. Syst.* **100**, 86–97 (2019). <https://doi.org/10.1016/j.future.2019.05.007>
- [9] Irfan, M., Dalai, S., Vishwakarma, K., Trslic, P., Riordan, J. & Dooly, G. Multi-sensor fusion for efficient and robust UAV state estimation. In *Proc. ICCMA* 35–40 (2024). <https://doi.org/10.1109/ICCMA63715.2024.10843888>
- [10] Yang, S., Luo, Y., Miao, W., Ge, C., Sun, W. & Luo, C. RF signal-based UAV detection and mode classification: A joint feature engineering generator and multi-channel deep neural network approach. *Entropy* **23**, 1678 (2021). <https://doi.org/10.3390/e23121678>
- [11] Zuo, M., Xie, S., Zhang, X. & Yang, M. Recognition of UAV video signal using RF fingerprints in the presence of WiFi interference. *IEEE Access* **9**, 88844–88851 (2021). <https://doi.org/10.1109/ACCESS.2021.3089590>
- [12] Ezuma, M., Erden, F., Anjinappa, C. K., Ozdemir, O. & Guvenc, I. Detection and classification of UAVs using RF fingerprints in the presence of Wi-Fi and Bluetooth interference. *IEEE Open J. Commun. Soc.* **1**, 60–76 (2020). <https://doi.org/10.1109/OJCOMS.2019.2955889>
- [13] Medaiyese, O. O., Ezuma, M., Lauf, A. P. & Adeniran, A. A. Hierarchical learning framework for UAV detection and identification. *IEEE J. Radio Freq. Identif.* **6**, 176–188 (2022). <https://doi.org/10.1109/JRFID.2022.3157653>
- [14] Medaiyese, O. O., Ezuma, M., Lauf, A. P. & Guvenc, I. Wavelet transform analytics for RF-based UAV detection and identification system using machine learning. *Pervasive Mob. Comput.* **82**, 101569 (2022). <https://doi.org/10.1016/j.pmcj.2022.101569>
- [15] Alhazbi, S., Sciancalepore, S. & Oligeri, G. The day-after-tomorrow: On the performance of radio fingerprinting over time. In *Proc. ACSAC* 439–450 (2023). <https://doi.org/10.1145/3627106.3627192>
- [16] He, J., Huang, S., Chang, S., Wang, F., Shen, B.-Z. & Feng, Z. Radio frequency fingerprint identification with hybrid time-varying distortions. *IEEE Trans. Wirel. Commun.* **22**, 6724–6736 (2023). <https://doi.org/10.1109/TWC.2023.3245070>
- [17] Zheng, H. & Gao, N. DRFF-R2: Multi-Scenario UAV Radio Frequency Signal Dataset. Science Data Bank (2026). <https://doi.org/10.57760/sciencedb.36815>.